

## Influence of Cu impurities and surface temperature to the formation of thin a-C:H(Me) film

Z. Rutkuniene

*Kaunas University of Technology, Physics department, Studentu 50,  
LT 51368, Kaunas, Lithuania,  
e-mail: zivile.rutkuniene@ktu.lt*

The aim of this experimental work is identify most important physical and chemical processes on the surface during amorphous carbon films formation on the silicon surface with copper nanoclusters (Cu). Duration of films deposition on n type silicon (100) surface by using different substrate temperatures (25 °C, 100 °C and 250 °C) was 45s. Velocity of film growth from C<sub>2</sub>H<sub>2</sub> gas plasma depended on surface temperature and was variable (0.2-0.5 nm/s). Data of null ellipsometry, Raman spectroscopy and element analysis showed that formation of amorphous carbon film is in the early stage and mixture of Si-C, Si-COH and GLC fragments is dominant on the surface. The experimental RS curves were fitted by few Gaussian-shape lines in the spectral range from 500 cm<sup>-1</sup> to 700 cm<sup>-1</sup>, from 700 cm<sup>-1</sup> to 900 cm<sup>-1</sup>, from 900 cm<sup>-1</sup> to 1100 cm<sup>-1</sup> and from 1100 cm<sup>-1</sup> to 1900 cm<sup>-1</sup> and analysis of the additional peaks in all ranges confirmed complexes of different carbons structures in the film. Carbon films with more ordered C-C bonds grows during film formation at higher temperatures (>100° C) on the silicon surface with Cu particles, because atoms of copper penetrate into the deeper layers of silicon. The substrate temperature influenced the surface amorphisation because of active oxygen and hydrogen diffusion into deeper layers and formation of hydrogenated silicon carbon with fragments of amorphous carbon films becomes not significant.

**Key words:** amorphous carbon films, metal impurities, Raman spectroscopy.

**PACS numbers:** 68.37.-d, 68.90.+g.

### Introduction

The insertion of metallic phase into the a-C: H matrix improves its mechanical performance and also gives the rise to new material properties [1]. Carbon films with metal impurities are interesting because of applicable in medicine like toxins of microorganisms [2] or in microelectronics as single electron devices [3]. Early stage of amorphous carbon film with or without metal impurities formation is interestingly because single theory of this process not is in nowadays. The few theoretical models is dominant: complete condensation, growth with re-evaporation, nucleation on defects, and total or null cluster-cluster coalescence [4]. It is known, that particles of metals on the surface catalyzed growth of nanoformation during amorphous carbon films deposition. One of the earliest mechanism for CNT growth proposed A. These and others, and it is the so-

called “scooter mechanism” [5], where metal atoms with high electronegativity chemisorbs to the open edge of a curving graphene sheet. It avoids formation of an endohedral fullerene and rearrange of carbon rings. Other mechanisms explaining the CNT growth using metal or non-metal catalyst exist also [6-8], but two of them are most acceptable: tip-growth model and base growth model. Interaction between catalyst particle and surface determined which of them would be dominant. Type of nanoformation (single or multy wall carbon nanotube, fullerene et. all) depends on the catalyst size [9]. Surface temperature is other important factor for nanostructure growth. High temperature is the reason for nanoclustering [10] because graphite like carbon films will forms on the surface during deposition in these conditions. Type of nanoformation (single or multy wall carbon nanotube, fullerene and other) depends on the catalyst size [9]. High temperature is the reason for nano-

clustering [10, 11] because graphite like carbon films will form on the surface during deposition in these conditions [12]. Formation of graphite like carbon film at comparative low temperatures is possible using PECVD methods, so addition of metals particles can be reason of nanostructures growth. Influence of metal additions and temperature to the properties of thin amorphous carbon films and possibilities of nanostructures formation are analyzed in this experimental work. The aim of it is to identify of most important physical and chemical processes on the surface during thin amorphous carbon films formation on the silicon surface with metals clusters (Cu) by PECVD method.

### Experimental setup

a-C: H films were formed on silicon surface with copper clusters by PECVD method using  $C_2H_2$  gas plasma. The temperature of silicon substrate was 25 °C, 100 °C and, 250 °C. Duration of deposition was 45 s bombarding ion energy was 200 eV. The copper was deposited before carbon film formation during bombardment the copper net by argon ions with ion energy 500 eV, deposition duration 20 min. The deposition and film formation took place in a single two steps technological process. The films optical properties were determined by null-ellipsometry (Gaertner L117 with a He-Ne laser (632.8 nm)), Raman spectroscopy (Ivon Jobin spectrometer with a Spectra Physics YAG: Nd laser (532.3 nm, 50 mW, spot size 0.32 mm)). The experimental RS curves were fitted by few Gaussian-shape lines in the spectral range from 500  $cm^{-1}$  to 700  $cm^{-1}$ , from 700  $cm^{-1}$  to 900  $cm^{-1}$ , from 900  $cm^{-1}$  to 1100  $cm^{-1}$  and from 1100  $cm^{-1}$  to 1900  $cm^{-1}$ . The relative element concentrations were measured by Bruker AXS Microanalysis GmbH.

### Results

The main properties of films and peaks values of Raman spectra are shown in the table 1 and the table 2. Deposition rate depended on the nature of metal clusters and substrate temperature (0.2 -0.5 nm/s). Differences in the Raman spectra at 25 °C are shown in the figure 1 (Raman shift range is 500  $cm^{-1}$  – 700  $cm^{-1}$ ) and figure 2 (range 1100  $cm^{-1}$  – 1800  $cm^{-1}$ ). Refractive index of all films is more typical polymer like films with high concentration of hydrogen and  $sp^2$  bonds because extinction coefficients also are

very high. It is important that silicon surface after Me clusters deposition is destroyed and activated during ion bombardment, so boundary line between silicon and amorphous carbon film is not clear. Inter-layer becomes most important and quantity of various bond of silicon with carbon, hydrogen or oxygen are influencing to the Raman spectra form.

**Table 1** – Main properties of a-C:H film with Cu impurities (thickness of film, refraction index, relative concentration of elements in the structure a-C:H/Cu/Si)

Substrate temperature	T=25°C	T=100°C	T=250°C
Thickness d, nm	22	18	12
Refraction index n	1.44	1.6	1,7
Carbon, at. %	14.4	10.3	5.7
Oxygen, at. %	8.3	6.5	5.6
Silicon, at. %	76,6	82,1	87,5
Copper, at. %	0.7	1.1	1.2

The peaks at 517  $cm^{-1}$ , 561  $cm^{-1}$ , 617  $cm^{-1}$  and 669  $cm^{-1}$  were obtained in the Raman spectra range from 500  $cm^{-1}$  to 700  $cm^{-1}$  when amorphous carbon films were deposited on the silicon surface with Cu clusters at the room temperature. The peak at 517  $cm^{-1}$  associated with silicon substrate but it shifts to the lower value when surface temperature increased (516  $cm^{-1}$  at 100 °C and 509  $cm^{-1}$  at 250 °C). Shifting of the silicon peak to lower values corresponds with the process of amorphization and intensity of it depends on substrate temperature [13]. Existing peak at 532  $cm^{-1}$  -535  $cm^{-1}$  correlate with the strain in the silicon [14] and at the higher temperature it become more intensive. The next two peaks in this range (561  $cm^{-1}$  and 617  $cm^{-1}$ ) are related with  $Cu_2O$  because this compound have three characteristic vibrations: at 570  $cm^{-1}$ , 618  $cm^{-1}$  and 624  $cm^{-1}$  [15]. Intensities of that are variable and depend on the temperature: the third peak is weak and is not fixed in the spectra when substrate temperature is 25 °C and 250 °C, but becomes dominant at 100 °C. Intensity of the second peak (617  $cm^{-1}$ ) decreasing at 100 °C, but it is dominant and shifted to the lower values (614  $cm^{-1}$ ) at 250 °C when other two peaks disappear. Variations of these peaks show dependence of structure and concentration of

cooper bonds with oxygen in the film and interlayer on the surface temperature. Wide peak at  $669\text{ cm}^{-1}$  is related to the Si-O-Si stretching [16] and its shift

to the lower values with the temperature increasing is conditioned by the bond deformation or deficiency of oxygen.

**Table 2 a** – C:H(Me) film peaks values of Raman spectra

Vibration modes	Peaks n RS spectra of the films, $\text{cm}^{-1}$	References	
Si-Si TO mode	509-518;	520;	[13]
Strain in Silicon	533; 535;	537	[14]
$\text{Cu}_2\text{O}$	570; 614; 617; 623;	570; 618; 624;	[15]
SiOH	586-610;	606;	[16]
Symmetric Si-O-Si stretching	664-669;		
Si- $\text{CH}_3$ rocking	690;	687;	[17]
Si-C	682; 732; 784;		[18]
	763-765;		[19]
	809-813;		[20]
	841, 874;		
	855;		
C-H	1036-1037; 1079;		[21]
Oxyethylene ring deformation	1122;		[22]
D4	1181-1197;	$\sim 1190$ ;	[23]
C-O-C stretching	1247;	1252;	[24]
C-C inter-ring stretching	1288;	1286;	[25]
D peak	1313-1396;	1350;	[26]
Transpolyacetylene $\nu_3$ C=C stretching mode	1410-1454;	$\sim 1450$ ;	[25]
Semicircle stretch vibrations in benzene or benzene clusters	1484;	1486;	[26]
G peak ( $E_{2g}$ symmetry)	1510-1553;	1550;	[23]
D' (G2 mode)	1611-1637;	1620;	[26, 27]
C=O stretching	1713-1788;	1680-1820;	[28]

The characteristics peaks for hydrogenated amorphous silicon (SiOH) ( $586\text{ cm}^{-1}$  and  $639\text{ cm}^{-1}$ ) and Si-C ( $682\text{ cm}^{-1}$ ) becomes more intensive in the spectra when the substrate temperature is  $100\text{ }^\circ\text{C}$ , but peak of Si-O-Si is less intensive. It means that competition of processes hydrogenation and oxidation of silicon is very important for interlayer formation of the early stage film deposition when substrate temperature increase.

The peak at  $732\text{ cm}^{-1}$  associated with O-C-O bonds in plane bending or  $\text{CH}_2$  in rocking mode is obtained in the spectra range of  $700\text{ cm}^{-1} - 900\text{ cm}^{-1}$  for samples with Cu impurities. This range is typical for silicon carbide. Most likely that this peak is related with amorphous SiC because other peaks

characteristic for it at  $763\text{ cm}^{-1}$ ,  $784\text{ cm}^{-1}$ ,  $809\text{ cm}^{-1}$ ,  $841\text{ cm}^{-1}$  and  $874\text{ cm}^{-1}$  were obtained also. Their intensity decreased with increasing temperature and it show that structure of silicon carbide becomes more orderly because weak peak of crystalline SiC at  $855\text{ cm}^{-1}$  is defined in the spectra. It is important that peaks related with C-H bonds deformation at  $750\text{ cm}^{-1}$  (also peaks at  $1037\text{ cm}^{-1}$  and  $1079\text{ cm}^{-1}$  in the RS range of  $1000\text{ cm}^{-1} - 1800\text{ cm}^{-1}$ ) becomes more intensive with increasing temperature. And it confirms that the oxygenation becomes less intensive than the hydrogenation of silicon or carbon when temperature of surface increases.

Typical asymmetric curve for amorphous carbon films was not obtained in the Raman spectra range at

1000  $\text{cm}^{-1}$  to 1800  $\text{cm}^{-1}$ . The separate peaks at 1197  $\text{cm}^{-1}$ , 1313  $\text{cm}^{-1}$ , 1409  $\text{cm}^{-1}$ , 1510  $\text{cm}^{-1}$ , 1552  $\text{cm}^{-1}$ , 1611  $\text{cm}^{-1}$  and 1738  $\text{cm}^{-1}$  are identified in the spectra of samples deposited in the 25 °C. First of them together with peak at 1409  $\text{cm}^{-1}$  can be related to the vibration of transpolyacetylene carbon groups, but confirmation of it is complicated because other authors [22] demonstrate that intensity of these peaks increase with increasing of hydrogen concentration in the plasma and it is not typical for transpolyacetylene. So, the peak at 1197  $\text{cm}^{-1}$  can be attributed to any known  $\text{sp}^2$  – related feature also, so in agreeing with the other authors it was remarked that this peak shows highly defective graphitic structure relaxes through the formation of occasional four-coordinated atoms between the planes [29, 30].

So, the shift to the lower values with increasing of the surface temperature is related with increasing of order in the graphitic structure, the relaxing of internal stress and the decreasing of defect. Some authors peak at 1450  $\text{cm}^{-1}$  ascribe to fullerene-like structures [31]. Confirmation of it is formation of these structures during longer time (300 s) deposition at the same experimental conditions [32]. It was obtained that this peak shifted to higher values with increasing temperature of samples and becomes equal to 1453  $\text{cm}^{-1}$  at 250 °C. Other peaks at 1510  $\text{cm}^{-1}$ , 1552  $\text{cm}^{-1}$ , 1611  $\text{cm}^{-1}$  can be attributed to variation of G band.

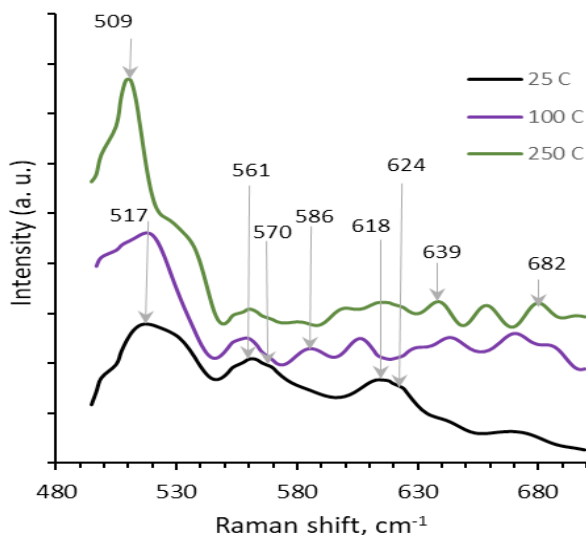


**Figure 1** – The Raman spectra of the a-C:H film with Cu impurities in the range from 500  $\text{cm}^{-1}$  to 700  $\text{cm}^{-1}$

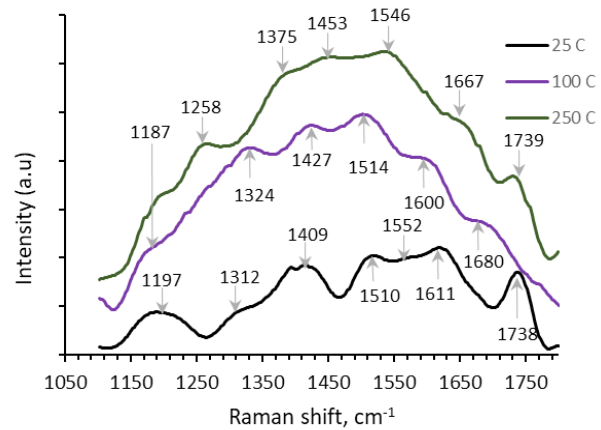


**Figure 2** – The Raman spectra of the a-C:H film with Cu impurities in the range from 1100  $\text{cm}^{-1}$  to 1800  $\text{cm}^{-1}$

Peak at 1611  $\text{cm}^{-1}$  is dominated when temperature of surface is 25 °C and it can be related with D' or G2 mode because the tangential G-band (at  $\sim 1580 \text{ cm}^{-1}$ ), which derived from the graphite-like in-plane mode, can split into several modes where two are the most distinct: G1 (1577  $\text{cm}^{-1}$ ) and G2 (1610  $\text{cm}^{-1}$ ) [33]. This splitting was also observed in the other papers [33-35].

The peak at 1738  $\text{cm}^{-1}$  comes from C=O stretching vibration and is intensive at low temperature. It confirmed that SiCOH groups formed on the surface. This peak becomes weak at 100 °C substrate temperature, but it arises becomes more intensive in the spectra at 250 °C.

## Discussion

EDS analysis shows, that initial concentration of Cu is same (1.2%) for all samples but films thickness and growth velocity decreased with increasing of sample temperature. Theoretically, only relative concentrations of carbon and silicon will depend on the film thickness, but copper concentration will remain same because copper clusters are in the interlayer and depths of EDS measurement are constant. But experimental results show that copper concentration also depends on surface temperature and it increased with temperature increasing. So, it is reason for assumption that copper can be removed from the surface because of desorption or ion bombardment during film deposition at 200 eV ion energy and 25 °C temperature. For that reason concentration of copper become,

lower (0.8%) and traces of copper oxides were obtained in the RS spectra. From another side, copper diffused into the deeper layers using silicon defects when substrate temperature is 100 °C. Concentration of it become lower in the film, but not in the film/interlayer/substrate structure and EDS measurements shows that total Cu concentration is higher (1.16%) but intensity of copper oxides peaks becomes lower in the Raman spectra. Peaks of  $\text{Cu}_2\text{O}$  disappears, but relative concentration of Cu remain similar (1.18%) when temperature increases till 250 °C and it show that diffusion process becomes more intensive at higher temperature. Amorphisation of silicon confirms these assumptions (shift of the silicon peaks into the lower values at higher temperatures, table 2). Single peak at  $614\text{ cm}^{-1}$  remains in the RS spectrum at highest temperature case, but it not related with copper oxide because other additional peaks not exist there. Also single similar peaks at  $613\text{ cm}^{-1}$  –  $617\text{ cm}^{-1}$  were obtained in the samples with Ag and Au [32], so it was decided that this peak is attributed to the C–C–C deformation in-plane vibration [36].

Analysis of the RS spectra in the other ranges shows that hydrogen remains in the forming film while Cu atoms bonds with oxygen and only part of it penetrate into the silicon substrate at low temperature. Slow film formation and more intensive penetration of hydrogen and oxygen into the silicon at higher temperatures create condition for hydrogenated silicon carbide formation. More intensive peaks related with Si-H, Si-C and Si-O and obtained in the spectra confirm this assumption. It is important also, that typical for the amorphous hydrogenated carbon films D and G modes in the spectra have low

intensities and it shows that a-C:H films is in early stage formation at low temperature. C-C bond become more ordered when temperature increased and it conditioned that thickness of this ordered film decreased. Measurement of refracting indexes also confirms these assumptions. Low refractive index (1.4) of films deposited at 25 °C is more characteristic for SiCOH films formed by PECVD method [37] than amorphous carbon film. Refractive index increased with temperature increases and becomes  $\sim 1.6$  at 250 °C. Featureless visible Raman spectra with no clear Raman peaks shows that films becomes polymer like (PLC) with low Young modulus ( $\leq 20\text{ GPa}$ ) and low density ( $\leq 1,2\text{ g/cm}^3$ ) [38].

### Conclusions

Formation of hydrogenated silicon carbon with fragments of amorphous carbon films on the silicon surface was obtained during early stage of a: C-H films deposition by PECVD methods. Carbon films with more ordered C-C bond grows during film formation at higher temperatures ( $>100^\circ\text{ C}$ ) on the silicon surface with Cu particles, because atoms of copper penetrate into the deeper layers of silicon. Amorphisation of substrate increases also. Lower refractive index than typical amorphous carbon films confirmed that the films deposited at 25 °C is more characteristic for SiCOH films. The typical for the amorphous hydrogenated carbon films D and G modes in the spectra have low intensities when films were formed at low temperature. More polymer like films forms at higher temperatures of the substrate.

### References

1. Kukielka S., Gulbiński W., Pauleau Y., Dub S.N. and Grob J.J. (2007). Nickel/Hydrogenated amorphous carbon composite films deposited in acetylene/argon microwave plasma discharge. *Reviews on advanced materials science*, 15, 127 – 133.
2. Ivanov-Omskii V.I., Panina L.K., Yastrebov S.G. (2000). Amorphous hydrogenated carbon doped with copper as antifungal protective coating. *Carbon*, 38, 495-499
3. Kolobov A.V., Oyanagi H., Akinaga H., Zvonaryova T.K. and Ivanov-Omskii V.I. (2000). Copper and cobalt nanoclusters embedded in hydrogenated amorphous carbon: an X-ray absorption study. 8th Int. Symp. „Nanostructures: Physics and Technology“, St.Peterburg, Russia, 299-303
4. Jensen P. (1999). Growth of nanostructures by cluster deposition: Experiments and simple models. *Reviews of Modern Physics*, 71, 1695–1735
5. Thess A., Lee R., Nikolaev P., Dai H., Petit P., Robert J., Young H. Lee, Xu C., Kim S. G., Rinzler A. G., Colbert D.T., Scuseria G.E., Tomanek D., Fischer J.E., Smalley R.E.(1996) Crystalline Ropes of Metallic Carbon Nanotubes. *Science*, 273(5274), 483-487.

6. Hong G., Chen Y., Li P., Zhang J. (2012). Controlling the growth of single-walled carbon nanotubes on surfaces using metal and non-metal catalysts. *Carbon*, 50 (6), 2067-2082.
7. Ding F., Rosen A. and Bolton K. (2005). Dependence of SWNT growth mechanism on temperature and catalyst particle size: Bulk versus surface diffusion. *Carbon*, 43 (10), 2215-2217.
8. Tessonnier J.P., Su D.S. (2011). Recent progress on the growth mechanism of carbon nanotubes: a review. *ChemSusChem*, 4(7), 824-847.
9. Yellampalli Siva. (2011). *Carbon Nanotubes – Synthesis, Characterization, Applications*, SRM University, India
10. Mora E., Pigos J.M., Ding F., Yakobson B.I. and Harutyunyan A.R. (2008). Low-temperature single-wall carbon nanotubes synthesis: feedstock decomposition limited growth. *Journal of the American Chemical Society*, 130, 1-8.
11. Tailleur A., Achour A., Djouadi M.A., Le Brizoual L., Gautron E., Tristant P. (2012). PECVD low temperature synthesis of carbon nanotubes coated with aluminum nitride. *Surface & Coatings Technology*, 211, 18–23.
12. Fadzilah A.N., Dayana K., Ruso M. (2013). Fabrication and characterization of camphor-based amorphous carbon thin films. *Procedia Engineering*, 56, 743 – 749.
13. Ambrosone G., Basa D.K., Coscia U., Santamaria L., Pinto N., Ficcadenti M., Morresi L., Craglia L., Murri R. (2010). E-MRS Spring meeting 2009, Symposium B. Structural and electrical properties of nanostructured silicon/carbon films. *Energy Procedia*, 2, 3-7
14. Prakash R., Amirthapandian S., Phase D.M., Deshpande S.K., Kesavamoorthy R., Nair K.G.M. (2006). Study of ion beam induced mixing in nano-layered Si/C multilayer structures. *Nuclear Instruments and Methods in Physics Research Section B Beam Interactions with Materials and Atoms*, 37 (30), 283-288.
15. Gan Z.H., Yu G.Q., Tay B.K., Tan C.M., Zhao Z.W., Fu, Y.Q. (2004). Preparation and characterization of copper oxide thin films deposited by filtered cathodic vacuum arc. *Journal of Physics D: Applied Physics*, 37(1), 81-85.
16. Grigonis A., Rutkuniene Z. and Vinciunaite V. (2010). Different wavelength laser irradiation of amorphous carbon. *Acta Physica Polonica A*, 120 (1), Proceedings of the VIII International Conference ION 2010, Kazimierz Dolny, Poland, 26-29/
17. Bae S.C., Lee H., Lin Z., Granick S.(2005). Chemical imaging in a surface forces apparatus: confocal Raman spectroscopy of confined poly(dimethylsiloxane). *Langmuir*, 21(13), 5685-5688.
18. Wasyluk J., Perova T.S., Kukushkin S.A., Osipov A.V., Feoktistov N.A., Grudinkin S.A. (2010). Raman investigation of different polytypes in SiC thin films grown by solid-gas phase epitaxy on Si (111) and 6H-SiC substrates. *Materials Science Forum*, 645-648, 359-362.
19. Moumita Mukherjee (2011). *Silicon Carbide – Materials, Processing and Applications in Electronic Devices*, Rijeka, Croatia, 8-9.
20. Kuntumalla M.K., Ojha H., Srikanth V.S. (2013). Identification of  $\beta$ -SiC surrounded by relatable surrounding diamond medium using weak Raman surface phonons. *Bulletin of Materials Science*, Volume 36 (6), 1087-1090.
21. Casiraghi C., Piazza F., Ferrari A.C., Grambole D., Robertson J. (2005). Bonding in hydrogenated diamond-like carbon by Raman spectroscopy. *Diamond and Related Materials*, 14, 1098-1102.
22. Birrell J., Gerbi J. E., Auciello O., Gibson J.M., Johnson J. and Carlisle J.A. (2005). Interpretation of the Raman spectra of ultrananocrystalline diamond. *Diamond and Related Materials*, 14 (1), 86-92.
23. Schwan J., Ulrich S., Batori V., Ehrhardt H., Silva S.R.P. (1996). Raman spectroscopy on amorphous carbon films. *Journal of Applied Physics*, 80 (1), 440-447.
24. Ahmed M.H., J.A. Byrne. (2012). Effect of surface structure and wettability of DLC and N-DLC thin films on adsorption of glycine. *Applied Surface Science*, 258 (12), 5166–5174.
25. Ferrari A.C., Robertson J. (2001). Origin of the 1150  $\text{cm}^{-1}$  Raman mode in nanocrystalline diamond. *Physical Review B*, 63, 121405-12408.
26. Makarova T., Ricc M., Pontiroli D., Mazzani M., Belli M., and Goffredi A. (2008). Ageing effects in nanographite monitored by Raman spectroscopy. *Physica status solidi (b)*, 245(10), 2082–2085.
27. Pimenta M.A., Dresselhaus G., Dresselhaus M.S., Cancado L.G., Jorio A., Saito R. (2007). Studying disorder in graphite-based systems by Raman spectroscopy. *Physical Chemistry Chemical Physics*, 9, 1276–1291
28. Cong C., Yu T., Saito R., Dresselhaus G.F., Dresselhaus M.S. (2011). Second-Order Overtone and Combination Raman Modes of Graphene Layers in the Range of 1690-2150  $\text{cm}^{-1}$ . *ACS Nano*, 5 (3), 1600 –1605.
29. Ulrich J., Batori S., Ehrhardt V., and Silva. (1996). *Raman spectroscopy on amorphous carbon films*. *Journal of Applied Physics*, 80 (1), 440 – 447.
30. Beeman D., Silverman J., Lynds R. and Anderson M. (1984). Modeling studies of amorphous carbon. *Physical Review B*, 30 (2), 870-875.
31. Blank V.D., Denisov V.N., Kirichenko A.N., Kulnitskiy B.A., Martushov S.Yu., Mavrin B.N. and Perezhogin I. A. (2007). High pressure transformation of single-crystal graphite to form molecular carbon onions. *Nanotechnology*, 18, 345601-1-4.

32. Rutkuniene Z., Vigricaite L. and Grigonis A. (2014). Nanostructure Formation during Amorphous Carbon Films Deposition. *ACTA PHYSICA POLONICA A* Vol. 125, No. 6, 1303-1306
33. Zdrojek M., Gebicki W., Jastrzebski C., Melin T., Huczko A. (2004). Studies of Multiwall Carbon Nanotubes Using Raman Spectroscopy and Atomic Force Microscopy. *Solid State Phenomena*, 99-100, 265-268.
34. Rao A.M., Ritcher E., Bandow S., Chase B., Eklund P.C., Williams K.A., Fang S., Subbaswamy K.R., Menon M., Thess A., Smalley R.E., Dresselhaus G., Dresselhaus M.S. (1997). Diameter-Selective Raman Scattering from Vibrational Modes in Carbon Nanotubes. *Science*, 275 (5297), 187-191.
35. Duesberg G.S., Loa I., Burghard M., Syassen K., and Roth S. (2000). Polarized Raman spectroscopy on isolated single-wall carbon nanotubes. *Physical Review Letters*, 85 (25), 5436-5439.
36. Nguyen B., Thu Vu T.K., Nguyen Q.D., Nguyen T.D., Nguyen T.A., Trinh T.H. (2012). Preparation of metal nanoparticles for surface enhanced Raman scattering by laser ablation method. *Advances in Natural Sciences: Nanoscience and Nanotechnology*, 3(2), 025016.
37. Park J.-M., Rhee Sh.-W. (2002). Remote plasma-enhanced chemical vapour deposition of nanoporous low-dielectric constant SiCOH films using vinyltrimethylsilane. *Journal of the Electrochemical Society*, 149(8), F161–F170.
38. Casiraghi C., Piazza F., Ferrari A.C., Grambole D., Robertson J. (2005). Bonding in hydrogenated diamond-like carbon by Raman spectroscopy. *Diamond and Related Materials*, 14, 1098-1102.